VHF, UHF and microwave frequency nanomechanical resonators

X M H Huang[1,3], **X L Feng**[1], **C A Zorman**[2], **M Mehregany**[2] **and M L Roukes**[1,4]

[1] Kavli Nanoscience Institute, Division of Engineering and Applied Sciences, Mail Code 114-36, California Institute of Technology, Pasadena, CA 91125, USA

[2] Department of Electrical Engineering and Computer Science, Case Western Reserve University, Cleveland, OH 44106, USA

E-mail: henry@nantero.com and roukes@caltech.edu

Abstract. Nanomechanical resonators with fundamental mode resonance frequencies in the very-high frequency (VHF), ultra-high frequency (UHF) and microwave L-band ranges are fabricated from monocystalline silicon carbide (SiC) thin film material, and measured by magnetomotive transduction, combined with a balanced-bridge readout circuit. For resonators made from the same film, we measured the frequency dependence (thus geometry dependence) of the quality factor. We have seen a steady decrease of quality factor as the frequency goes up. This indicates the importance of clamping losses in this regime. To study this source of dissipation, a free-free beam SiC nanomechanical resonator has been co-fabricated on the same chip with a doubly clamped beam resonator operating at similar frequencies. Device testing has been performed to directly compare their characteristics and performance. It is observed that a significant improvement in quality factor is attained from the free-free beam design. In addition, from studies of resonators made from different chips with varying surface roughness, we found a strong correlation between surface roughness of the SiC thin film material and the quality factor of the resonators made from it. Furthermore, we experimentally studied the eddy current damping effect in the context of magnetomotive transduction. A high-aspect ratio SiC

---

[3] Current address: Nantero, Inc., 25-D Olympia Ave, Woburn, MA 01801, USA.

[4] Author to whom any correspondence should be addressed.
Some preliminary results to those described herein were presented at the *Transducers' 03 conference*.

nanowire resonator is fabricated and tested for this study. Understanding the dissipation mechanisms, and thus improving the quality factor of these resonators, is important for implementing applications promised by these devices.

Contents

1. Introduction

Doubly clamped beam resonators based upon nanoelectromechanical systems (NEMS) with operating frequencies within the microwave L-band have recently been achieved [1], owing to both the development of better materials [2] and novel detection techniques [3]. This new breakthrough promises a broad range of applications, including next-generation high-resolution sensors and actuators, and high-speed signal processing components [4]–[8]. These devices also offer the potential advantage of much easier integration compared to current approaches. However, these first microwave NEMS resonators have exhibited decreasing quality factors as the device frequency is increased. If unaddressed, this could significantly restrict the range of applications for this developing technology. In this paper, after first describing important details about the fabrication and measurement of these NEMS devices, we summarize our initial attempts to address this important problem (section 4), as well as our efforts to improve the measurement techniques at these frequencies.

One of the possible reasons for the decrease of quality factor in these devices is the clamping loss intrinsic to the doubly clamped boundary condition [9, 10]. Nguyen and co-workers have previously demonstrated the use of a free-free boundary condition to reduce this source of acoustic loss for micromachined resonators [11, 12]. In section 5 of this paper, we describe our investigations into the application of the free-free beam design for nanoscale resonators, where the feature size is at least an order of magnitude smaller than that of their micromachined counterparts.

Surface roughness of the silicon carbide (SiC) thin film material may potentially affect the quality factor of the resonators made from it. In our experiments, resonators are fabricated from different precursor wafers that possess varying degrees of surface roughness. In section 6 of this paper, we describe a set of experiments in which the correlation between surface roughness of the SiC thin film employed and the resulting quality factor of the resonators is explored.

Finally, when magnetomotive displacement transduction is employed for device readout into the electrical domain, the eddy current damping effect [13] can become quite pronounced under certain conditions. Characterization of this effect is rather crucial for quality factor optimization of these resonators. In section 7, we describe our investigations of this phenomena based upon fabrication and measurement of high-aspect ratio SiC nanowire resonators to elucidate the eddy current damping mechanism, and to quantitatively measure this effect.
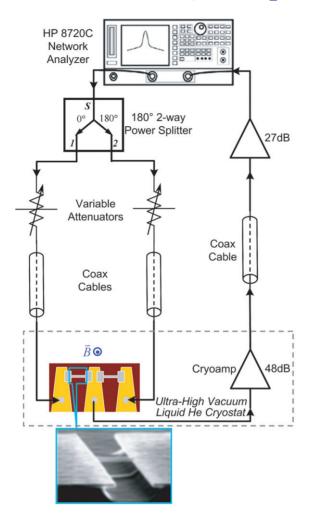
2. Nanofabrication

3C-SiC nanomechanical resonators are now routinely fabricated from epitaxially grown monocrystalline 3C-SiC layers, using a surface nanomachining technique that we have detailed elsewhere [2]. Here, we present optimization of the process for very-high frequency (VHF), ultra-high frequency (UHF) and microwave-frequency devices designed to operate at resonance frequencies above 100 MHz.
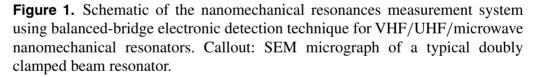
Briefly, the 3C-SiC films used in this work are heteroepitaxially grown on 100 mm diameter (100) Si wafers in an rf-induction-heated, atmospheric pressure chemical vapour deposition reactor [2]. SiH_4 and C_3H_8 are used as precursors, and H_2 is used as a carrier gas. The epitaxial process is a two-step, high-temperature (1280°C) procedure, involving the carbonization of the Si surface in a C_3H_8/H_2 ambient followed by epitaxial growth using SiH_4, C_3H_8 and H_2. The epitaxial growth recipe is optimized for micron-thick films, yet it produces 50–250 nm thick films of sufficient surface quality for e-beam lithography and subsequent nanomachining.

Device fabrication utilizes a combination of optical and electron beam lithography techniques. The process begins by using standard photoresist and optical lithography to define the large-area contact pads comprising a 4 nm thick Cr adhesion layer and an 80 nm thick Au film. The substrates are then coated with a PMMA thin film, which is then patterned by electron beam lithography into a metallic lift-off mold to define the submicron mechanical structures of the SiC devices. The pattern on the metal mask (typically ∼30 nm Al, followed by ∼5 nm Ti) is transferred to the 3C-SiC structural layer by using a $NF_3/O_2/Ar$ anisotropic etch with an electron cyclotron resonance (ECR) plasma etching system. The newly patterned 3C-SiC beams are then suspended by simply etching the underlying Si substrate using an isotropic NF_3/Ar ECR etch. The metal etch mask remains on the SiC beams to be used as a conducting layer for device testing.

The etch rate of SiC anisotropic etch is on the order of 100 nm min^{-1} (which depends on the power and bias settings for the plasma in ECR etch process, and the exact location of the sample in the plasma ambient), while the etch rate for the metallic mask is on the order of 1 nm min^{-1}. Such contrast in etch rate (high-etching selectivity) enables us to use very thin layer of metals, which is important in the fabrication of ultra-small devices.

For our typical VHF/UHF/microwave SiC nanomechanical resonators, we employ 30 nm of Al, followed by 5 nm of Ti as the choice for device metallization, even though other metals such as Au and Ni are also capable of surviving the ECR etching process and can provide the electrical conductivity required by the detection scheme to be discussed later in this paper. The low-mass density of Al helps in reducing mass loading, thus resulting in a higher frequency for the same device geometry as compared with a denser metal. The thin Ti top layer helps reduce oxidation of Al in the first ECR etching step, where oxygen is used as a gas component.

Figure 1. Schematic of the nanomechanical resonances measurement system using balanced-bridge electronic detection technique for VHF/UHF/microwave nanomechanical resonators. Callout: SEM micrograph of a typical doubly clamped beam resonator.

A typical suspended nanostructure is shown in the inset of figure 1. Two nearly identical suspended doubly clamped beam devices form a configuration for testing. Typical devices are made from $75 \sim 100$ nm thick SiC layers, with beam widths of $100 \sim 150$ nm and lengths of 1.0–$3.0 \, \mu$m, for operation in the VHF/UHF/microwave range. A typical beam device with appropriate metallization has a measured resistance of about $100 \, \Omega$ at room temperature, with the resistance mismatch between the two beams on the same sample to be within a few per cent.

3. Measurement of mechanical resonance

Device testing is performed in ultra-high vacuum (provided by liquid helium cooling of a sealed and evacuated cryostat) and involves the use of magnetomotive transduction [13, 14] in conjunction with a variation of the balancing technique [3] tailored for VHF/UHF/microwave applications.
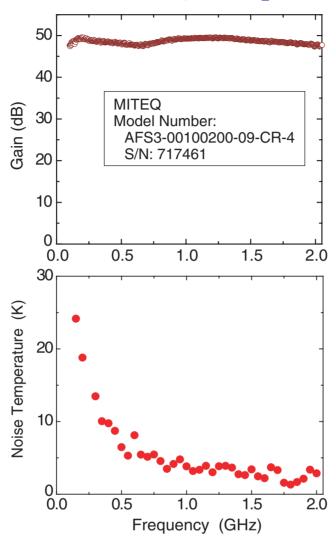
Figure 2. Measured gain and noise temperature of the cryogenic amplifier when it is immersed in liquid helium.

The schematic circuit diagram is shown in figure 1. The sample is positioned in a magnetic field with the beams perpendicular to the field lines. The potential of the centre pad is initially held at virtual ground by using a 180° power splitter to provide out-of-phase driving of the two device branches and by making the impedance of the two branches of the circuitry as close to identical as possible. The two beams are also nearly (but not exactly) identical to each other. As a result, they have slightly different resonance frequencies. When the drive frequency is swept to match the fundamental resonance frequency of one of the beams, resonant motion is induced to cut the field lines resulting in an electromotive force (EMF) voltage that can be detected. Nonidealities in the system produce a high-residual background, which can be reduced using the balanced-bridge technique, in comparison to a conventional reflection measurement scheme [3]. The improvement here is limited by the resistance mismatch (of a few per cent) in between the two beams, which was sufficient for this experiment. Further improvement can be made by using variable attenuators and adjustable phase shifters to further match the impedances of the two branches of the bridge circuit. The use of a low-noise cryogenic amplifier (measured characteristics shown in figure 2)
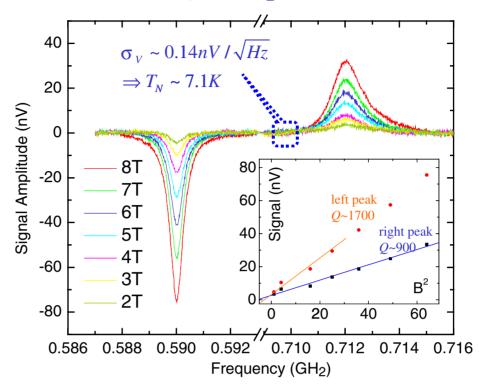
Figure 3. Measured electromechanical resonances from a typical pair of UHF nanomechanical resonators using the balanced-bridge detection scheme with magnetomotive transduction. Resonances detected as the B field sweeps from 1 to 8 tesla (with the background response at 0 tesla subtracted). The noise floor of detection is measured to be $\sim 0.14\,\text{nV}/\sqrt{\text{Hz}}$, or $\sim 7.1\,\text{K}$ in noise temperature. This is a combination of noise from cryoamp, and the Johnson noise from the metallic resistors on the resonator beams. Inset: the resonance peak amplitude is a quadratic function of the B field, as verified by the measured data from both the 590 MHz and the 712 MHz devices. Lorentzian fit of the de-embedded data traces give $Q \sim 1700$ for the 590 MHz resonance and $Q \sim 900$ for the 712 MHz peak.

enables the detection of displacements on the order of femtometers. Resonance curves at different B fields for a typical UHF resonator pair are shown in figure 3. The peak and the dip represent the resonance of each of the two doubly clamped beams, respectively. The observed noise temperature (referred back to the input of the amplifier) is about 7.1 K. The noise comes from a combination of amplifier noise and the Johnson noise due to beam resistance sitting at 4.2 K. The resultant noise temperature implies that the displacement detection sensitivity on the order of fm/$\sqrt{\text{Hz}}$ has been achieved in our experiments. The maximum signal amplitude depends linearly on B^2, as expected. The peaks are fitted to a Lorentzian curve to extract the quality factor, Q. Here, $Q = \omega_0/\Delta\omega$, where ω_0 is the resonance frequency and $\Delta\omega$ is peak width in power spectrum (i.e., width at half maximum signal power, or equivalently, $1/\sqrt{2}$ maximum signal amplitude).

Shown in table 1 is a collection of the basic specifications of a family of typical 3C-SiC doubly clamped beam nanomechanical resonators we have demonstrated.

Table 1. Basic specifications of 3C-SiC doubly clamped beam nanomechanical resonators operating in the VHF/UHF/microwave ranges.

Resonance frequency (MHz)	l (μm)	w (nm)	t (nm)	Device mass (fg)	Measured Q
190	2.35	150	100	145.0	5200
200	3.1	180	100	229.5	7500
241	1.8	150	100	111.1	1500
295	2.66	170	80	160.2	3000
339	1.6	140	75	71.3	3600
357	1.55	160	75	78.9	3000
395	1.75	120	80	74.4	2500
411	1.7	120	80	72.3	2500
420	1.8	150	100	111.1	1200
428	1.65	120	80	75.5	2300
480	1.32	140	75	61.3	1600
482	1.55	120	80	70.9	2000
488	1.31	150	75	60.8	1600
590	1.6	140	75	71.2	1700
712	1.55	160	75	78.9	900
1014	1.11	120	75	44.2	500
1029	1.09	120	75	43.4	500

4. Clamping loss

The frequency dependence of Q for a number of devices fabricated from the 3C-SiC film is plotted in figure 4. As virtually the same fabrication processes are used in making these devices, the beam length is the only parameter that changes significantly in scaling up the frequency, with the shortest beams ($\sim$1.1 μm) yielding the highest resonant frequencies. The steady decline in Q with increasing frequency for beams made from the same film suggests that the clamping loss mechanism may play a key role in determining the measured Q at VHF/UHF/microwave frequencies.

At least two approaches (or their combination) may be used to alleviate clamping loss at such frequencies. One is to further shrink the dimensions of the devices. To keep the same operating frequency, larger aspect ratio should be pursued, thus reducing clamping loss and improving Q, according to the results shown here. The other approach is the application of a free-free beam design, to support the beam at the motional nodal points of fundamental resonance, and strategically design the support structure to minimize energy transfer from the resonance mode to the environment. The free-free beam resonator design was initially pioneered by Nguyen and his co-workers, in their efforts of engineering high-Q micromechanical resonators [11, 12].

5. Free-free beam nanomechanical resonators

We implement the in-plane (lateral) free-free beam design strategy to our nanoscale mechanical resonators, to explore the possibility of reducing clamping loss. We fabricate pairs of devices consisting of a free-free beam and a doubly clamped beam, very close in designed
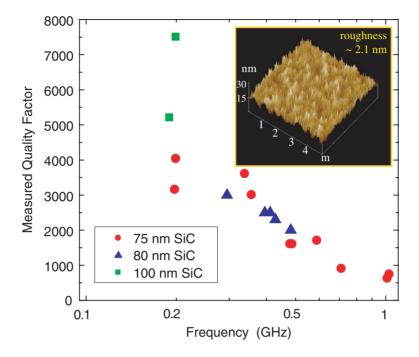
Figure 4. Measured quality factor versus resonance frequency for doubly clamped beam devices made from nominally $75 \sim 100$ nm thick 3C-SiC films. These devices are fabricated with essentially the same e-beam lithography, metallization and etching processes (typical beam metallization: 5 nm Ti atop of 30 nm Al; typical beam width: $120 \sim 150$ nm; beam length: $1.0 \sim 3.0\,\mu$m). The beam length is the major parameter that is rationally changed to scale the frequency from about 200 MHz up to over 1 GHz. Inset: a typical AFM scan of (80 nm) SiC film surface, from which some of these devices are made.

fundamental-mode resonance frequencies, for comparison in control experiments. Shown in figure 5(a) is an SEM image of a pair of these resonator devices.

The high-Q free-free beam nanomechanical resonators are first achieved in the VHF range. The test is performed by replacing this device pair into the circuit shown in figure 1. The variable attenuators are adjusted to improve balancing. The pair of resonator beams under test have a length of $\sim 3.0\,\mu$m, the width of resonator beams and support beams (in the free-free design) are both $\sim 0.15\,\mu$m. In-plane fundamental-mode resonances are observed at 170.01 and 174.59 MHz, respectively. By changing the variable attenuators and observing the amplitude change of both resonance peaks, we are able to determine that the 170.01 MHz peak is from the doubly clamped beam (figure 5(b)), while the 174.59 MHz peak is from the free-free beam resonator (figure 5(c)). Lorentzian fits to these peaks after de-embedded from the electrical background give us quality factors for these resonators. The quality factor of the doubly clamped beam is ~ 4500, whereas that of the free-free beam resonator is $\sim 11\,000$. The quality factor for the doubly clamped case is consistent with what we have observed in routinely fabricated and measured other doubly clamped beam resonators having similar geometric dimensions and made from the same SiC film or those having similar surface roughness. The free-free beam measured in this experiment has a quality factor significantly higher than the best value from its doubly clamped counterpart.
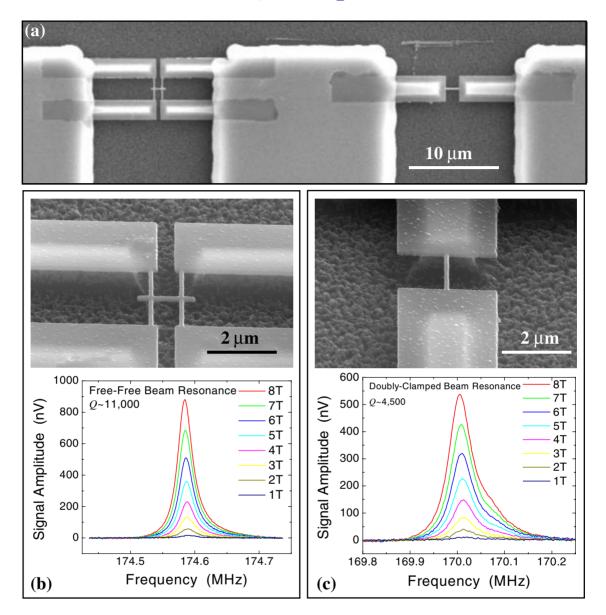
Figure 5. SEM micrographs and detected resonances of a typical co-fabricated pair of a free-free beam and a doubly clamped beam for the controlled experiment of studying the clamping loss in VHF/UHF SiC nanomechanical resonators. (a) Top view of a co-fabricated pair. (b) Zoom-in tilted view of the lateral free-free beam resonator and the measured mechanical resonance at different B field values. Lorentzian fit to these peaks gives a quality factor of $\sim$11 000. (c) Zoom-in tilted view of the doubly clamped beam resonator and the measured resonance, showing $Q \sim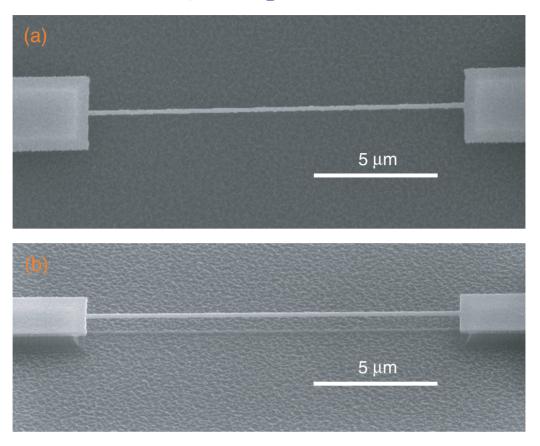 4500$. The quality factor from the free-free beam resonance is about 2.4 times that from the doubly clamped beam resonance.

Institute *of* **Physics** Φ DEUTSCHE PHYSIKALISCHE GESELLSCHAFT

Figure 6. SEM micrographs of a suspended high-aspect ratio SiC doubly clamped beam resonator (a top-down fabricated SiC nanowire), specifically designed for the study of eddy current damping effect. (a) Top view and (b) Tilted view of the device.

6. Effects from surface roughness

To investigate the effect of film quality on resonator performance, devices have been fabricated from films that differ significantly in surface roughness. A typical AFM image of SiC surface is shown in the inset of figure 4. In all cases, devices operational in the UHF/microwave regime are made from films that have a low-surface roughness ($\sim$2 nm or below). In contrast, devices made from rougher films (up to $\sim$7.1 nm) were operational in the VHF range, but not higher. Within the same apparatus and setup for detection and measurement, failure to detect any signal indicates an upper limit in the quality factor to be well below $\sim$100. These results suggest a strong correlation between quality factor and surface roughness.

The epitaxial growth recipe used to prepare the 3C-SiC films was initially designed for MEMS applications and thus was optimized for micron-thick films; yet it can produce 50–250 nm thick films of sufficient surface quality for e-beam lithography. Our results indicate that while the surfaces might be sufficient for fabrication purposes, it is critically important that the growth processes be optimized to produce ultra-smooth SiC thin films if these films are to be used for nanomechanical resonators having reasonably high-Q values. The issue of surface roughness is only now coming to the forefront, since until recently, nanomechanical beam resonators have
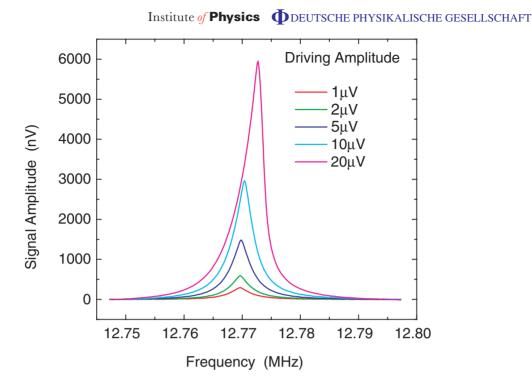
Institute *of* **Physics** Φ DEUTSCHE PHYSIKALISCHE GESELLSCHAFT

Figure 7. Resonance curves at different driving amplitudes measured from the high-aspect ratio SiC resonator (data taken at a constant *B* field of 6 tesla). The resonator approaches its nonlinear regime as the drive level keeps increasing, as expected to behave like a Duffing oscillator.

only been fabricated from Si wafers (bulk and SOI) and epitaxial III–V films (i.e., GaAs) that have ultra-smooth surfaces by virtue of a long history in microelectronics. This issue will also continue to be important as new materials are added to the NEMS toolbox in response to the widening array of applications. Recipes for growing ultra-thin SiC films optimized for surface smoothness, and techniques for SiC thin film surface polishing are currently under development. Some latest progress of these efforts is presented in [15].

7. Eddy current damping

The magnetomotive displacement transduction technique [3, 6, 13, 14, 16] has played a very important role in a series of recent achievements including the gigahertz SiC nanomechanical resonators [1] and the platinum nanowire resonators [17]. There has been tremendous interest in attempting to use this method for studying mechanical motion and resonance of single-walled nanotubes (SWNTs) [18], and molecular-scale electromechanical structures in general. However, the validity of this technique needs to be carefully examined and reassessed for experiments that push deep into the nanometre-scale size regime. As recently pointed out by Schwab [19], eddy current damping force caused by this transduction scheme may become important under certain experimental conditions. This damping mechanism has earlier been carefully studied by Cleland and Roukes [13] and is usually a small effect, but will become crucial for single molecules, such as an SWNT. Here, we have designed a high-aspect ratio SiC nanowire resonator to serve as a *dummy nanotube* to study this dissipation mechanism by simulating the situation to be faced by SWNTs.
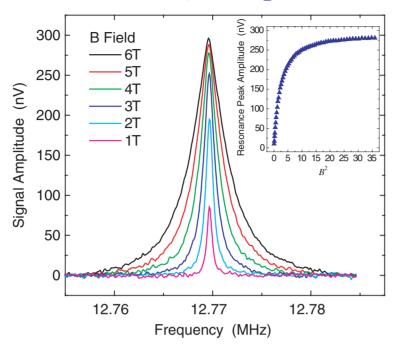
Figure 8. The eddy current damping effect—measured resonance curves at different B fields for the high-aspect ratio SiC resonator. Inset: the resonance peak amplitude as a function of B^2, which deviates significantly from the usual linear dependence (data taken at a constant driving amplitude of $1\,\mu V$).

In the magnetomotive transduction scheme, one relies on the EMF voltage generated by the motion to infer the action of the nanomechanical resonator. As pointed out by Cleland and Roukes [13], no additional dissipation is expected when the external impedance seen by the EMF voltage source is infinite. Of course, this is generally not the case for practical high-frequency measurements. As a result, eddy currents are present, in addition to the driving current, due to the EMF, thus generating an additional force, which is always opposed to, and tends to damp the motion of the beam and, hence leading to dissipation, and lowering the observed Q, as compared to the intrinsic one.

Assuming the dissipation processes are uncorrelated and additive, one can express the quality factor Q as

$$\frac{1}{Q} = \frac{1}{Q_M} + \frac{1}{Q_E} = \frac{1}{m\omega_0}(\beta_M + \beta_E), \tag{1}$$

where Q_M is the mechanical quality factor, β_M is the mechanical damping constant; Q_E, β_E are the partial quality factor and eddy current damping constant due to the loss from EMF induction [19], where β_E is defined as

$$\beta_E \equiv \frac{\partial I}{\partial V} B^2 l^2, \tag{2}$$

where I and V are current and voltage across the beam, l is the length of the beam. For low-operating frequencies, $\partial V/\partial I$ can be made large to minimize the effect. However, this
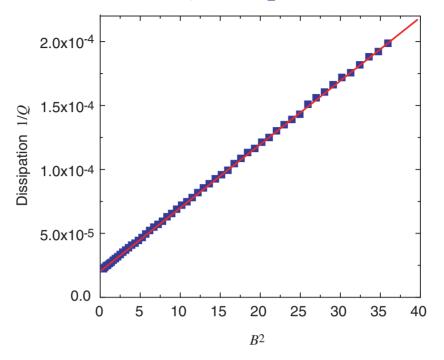
Figure 9. Measured dissipation ($1/Q$) in the high-aspect ratio (top-down nanowire) SiC resonator, as a function of B^2. The intercept of the linear fit gives the overall dissipation of the resonator without the eddy current damping effect, i.e., the theoretical limit of minimum dissipation can be achieved in magnetomotive transduction.

becomes not practical at high frequencies due to the unavoidable parasitic components in the electronic circuitry.

The doubly clamped beam nanowire resonator we use here is made from 3C-SiC thin film (75 nm thick), fabricated by top-down nanolithography method, with a process discussed earlier in this paper. The nanowire beam is about 15 μm long, 0.15 μm wide, with 45 nm Al, followed by 5 nm Ti on top as etch mask and metallization layer for electrical conduction. SEM micrographs of a typical suspended top-down nanowire device for this experiment are shown in figure 6.

The device is wire-bonded, loaded into a low-temperature vacuum cryostat which is then evacuated and cooled to liquid helium temperature. A strong magnetic field is applied perpendicular to the sample surface to allow magnetomotive actuation and detection. In-plane fundamental mode mechanical resonance is detected at 12.77 MHz. Figure 7 shows the resonance curve at different driving voltage, at a constant B field value of 6 tesla. At high driving forces, the device will perform as a standard nonlinear Duffing oscillator. This result enables us to choose a drive level, so as to work within the linear regime (dynamic range) of the resonator.

The driving voltage is chosen to be 1 μV, and the resonance curves at different B field are plotted in figure 8. The maximum amplitude versus B^2 is shown in the inset of figure 8, which differs significantly from a linear dependence found in the literature [2, 14]. It resembles linear dependence only at low-field values. Obviously, such deviation is due to the increase of dissipation at higher-B field values. Quality factor Q is experimentally determined by Lorentzian fits to the resonance curves.

Institute *of* **Physics** Φ DEUTSCHE PHYSIKALISCHE GESELLSCHAFT

Figure 9 is a plot of measured overall dissipation $1/Q$ with respect to B^2. The linear relation shown is as expected from equation (1). From the intercept of the linear fit, we can calculate that Q_M is about 50 000, which is the quality factor of the resonator without additional loss caused by the magnetomotive transduction scheme.

When we come to the point of experimenting with an actual single-walled carbon nanotube resonator, for example, of $1\,\mu$m long with doubly clamped boundary condition, eddy current damping is expected to be dominant at 8 tesla, making Q to be on the order of 100. As we reduce the B field to 1 tesla, Q should increase, and possibly approach the order of 10^4 (if other dissipation processes contribute much less than the eddy current damping at 1 tesla B field). This can be considered as a signature of nanotube motion to look for.

The sensitivity of such detection is limited by the first stage electrical amplifier noise, when the signal is optimally coupled to the amplifier. Nonideal coupling will reduce the sensitivity further, thus it is important to improve impedance matching between the device output and amplifier input.

8. Conclusions

In conclusion, we have demonstrated that the resonance frequency of SiC nanomechanical resonators designed to operate in the VHF and UHF to low microwave L-band ranges can be measured using magnetomotive transduction techniques. Dissipation according to clamping loss in such devices increases as the aspect ratio of these doubly clamped beams is reduced. We have demonstrated that the SiC free-free beam nanomechanical resonators offer significant improvement in quality factor compared to doubly clamped beam design operating at similar frequencies. By examining devices made from SiC wafers with different roughness, a strong correlation between surface roughness and quality factor is established from our experiments. Furthermore, the eddy current damping effect inherent to the widely used magnetomotive transduction scheme is experimentally measured using a top-down nanofabricated SiC nanowire device. This dissipation effect is particularly important for large aspect ratio beam resonators. Understanding the dissipation mechanisms and achieving the ability to improve the quality factors of such resonators are crucial for realizing high-Q nanomechanical resonators and thus important for a wide variety of potential applications promised by these devices.

Acknowledgments

References

[1] Huang X M H, Zorman C A, Mehregany M and Roukes M L 2003 *Nature* **421** 496
[2] Yang Y T, Ekinci K L, Huang X M H, Schiavone L M, Roukes M L, Zorman C A and Mehregany M 2001
       Appl. Phys. Lett. **78** 162
[3] Ekinci K L, Yang Y T, Huang X M H and Roukes M L 2002 *Appl. Phys. Lett.* **81** 2253
[4] Roukes M L 2001 *Sci. Am.* **285** 48
[5] Roukes M L 2001 *Phys. World* **14** 25

[6] Cleland A N and Roukes M L 1998 *Nature* **392** 160
[7] Nguyen C T C, Katehi L P B and Rebeiz G M 1998 *Proc. IEEE* **86** 1756
[8] Carr D W, Evoy S, Sekaric L, Craighead H G and Parpia J M 1999 *Appl. Phys. Lett.* **75** 920
[9] Lifshitz R 2002 *Physica* B **316** 397
[10] Cross M C and Lifshitz R 2001 *Phys. Rev.* B **64** 085324
[11] Wang K, Wong A C and Nguyen C T C 2000 *J. Microelectromech. Syst.* **9** 347
[12] Hsu W T, Clark J R and Nguyen C T C 2001 *Digest of Technical Papers, the 11th Int. Conf. on Solid State Sensors & Actuators (Transducers '01 and Eurosensor XV) Munich, 10–14 June 2001* (Munich: Springer) p 1110
[13] Cleland A N and Roukes M L 1999 *Sensors Actuators* **72** 256
[14] Cleland A N and Roukes M L 1996 *Appl. Phys. Lett.* **69** 2653
[15] Fu X A, Zorman C A and Mehregany M 2004 *J. Electrochem. Soc.* **151** G910
[16] Harrington D A 2003 *PhD Thesis* California Institute of Technology, Pasdena, CA
[17] Husain A, Hone J, Postma H W C, Huang X M H, Drake T, Barbic M, Scherer A and Roukes M L 2003 *Appl. Phys. Lett.* **83** 1240
[18] Saito R, Dresselhaus G and Dresselhaus M S 1998 *Physical Properties of Carbon Nanotubes* (London: Imperial College Press)
[19] Schwab K 2002 *Appl. Phys. Lett.* **80** 1276